Instantaneous fabrication of arrays of normally closed, adjustable, and reversible nanochannels by tunnel cracking

K. L. Mills,[a] Dongeun Huh,[b] Shuichi Takayama,*[b,c] and M. D. Thouless*[a,d]

Received (in XXX, XXX) Xth XXXXXXXXX 200X, Accepted Xth XXXXXXXXX 200X
First published on the web Xth XXXXXXXXX 200X
DOI: 10.1039/b000000x

A direct fabrication method capable of producing fully-reversible, tuneable nanochannel arrays, without the use of a molding step, is described. It is based on tunnel cracking of a readily-prepared brittle layer constrained between elastomeric substrates. The resulting nanochannels have adjustable cross-sections that can be reversibly opened, closed, widened and narrowed merely by applying and removing tensile strains to the substrate. This permits reversible trapping and release of nanoparticles, and easy priming or unclogging of the nanochannels for user-friendly and robust operations. The ease of fabrication and operation required to open and close the nano-channels is superior to previous approaches.

Introduction

Nanofluidics research encompasses a broad range of topics within chemistry, biology, and physics. Some of the research being pursued includes the separation or sorting of molecules based on size[1] or chemical affinity[2], and high-fidelity fluorescence detection[3]. Furthermore, there is considerable interest in the controlled confinement and manipulation of single molecules including several studies on the manipulation and elongation of DNA molecules in nanochannels[4-8].

Conventional nanofabrication techniques[9, 10] often consist of multiple steps involving costly equipment. Consequently, a surge in alternative nanofabrication techniques for creating nanochannels has occurred recently. These are generally aimed at alleviating the high costs associated with traditional nanofabrication techniques so that the devices may either be mass produced or generated easily in an academic setting. The new methods often introduce a variation to an existing micro- or nano-fabrication method, for example, soft-lithography: nanochannels have been made by molding poly-(dimethylsiloxane) (PDMS) over a network of electrospun polyethylene oxide fibers which are then etched away[11]. As a slight variation on nanoimprint lithography, the profile of drawn silica wires has been transferred to the surface of a thermoplastic by hot embossing[12]. Other methods make use of surface phenomena such as adhesive[13] or forced[14] collapse of larger structures to minimize a cross-sectional area to the nano-scale. Another surface phenomenon, the regular buckling pattern of a stiff, surface-modified layer on a compliant substrate[15], has also been used to form nanochannels[16].

In some cases, the new methods allow for capabilities that cannot be realized using traditional techniques. Recently, we reported a fabrication method, based on the fracture of a surface-modified layer, to create adjustable nanochannels in the compliant elastomer PDMS[17]. Soft-lithography techniques[18] were employed to create nanofluidic devices through two successive molding steps (with an inverse replica master bonded to a patterned half of the device). The nano-channels were formed in the open state, but could be closed by squashing the stucture. Careful control of the PDMS formulation and nano-channel surfaces was required to ensure that the channels would open again upon removal of the compressive load. Manipulation of nanoparticles and triggering confinement-induced elongation of DNA molecules by closing the nano-channels was demonstrated[17]. However, the method of nanochannel modulation was cumbersome as compressive loads had to be applied directly to the surface of the device.

Here, we present a new method to produce size-adjustable nanochannels in an even more direct and simple fashion. This approach is based on the mechanics associated with the tunnel cracking of a stiff, brittle layer sandwiched between compliant, tough substrates subjected to an applied tension. Subsequent relaxation and re-application of the tension that created the nanochannels can be used to induce reversible changes in the cross-sectional dimensions of the nanochannels. The applied tension can be readily varied in a continuous fashion and at different rates. This new method for fabricating arrays of nanochannels that are closed in their natural state but readily open upon application of a strain is particularly advantageous because control of a remote tensile strain is much easier than control of the compressive force required for our previous system[17]. Furthermore, this approach eliminates the possibility that a nanochannel will remained closed under the influence of surface forces.

Experimental Section

Nanochannel Fabrication and Characterization

The device consisted of a slab containing two microchannels (width = 100 μm, height = 50 μm) spaced 1 mm apart and a featureless film (~160 μm thick), both cast from PDMS (Dow Sylgard 184) and cured at 60°C for 12-15 hours (Fig. 1). The slab and thin film were cleaned and placed in a vacuum (40-60 mTorr) for 10-20 minutes prior to exposure to plasma oxygen for 60 minutes (Harrick Plasma, 30 W). The exposed

surfaces were then placed in contact with one another which led to spontaneous permanent bonding[19, 20]. The bonded system was loaded into a stretcher, and a uniaxial tensile strain was applied to introduce cracks within the bonded layer. Additional fabrication details may be found in the Supplementary Information.

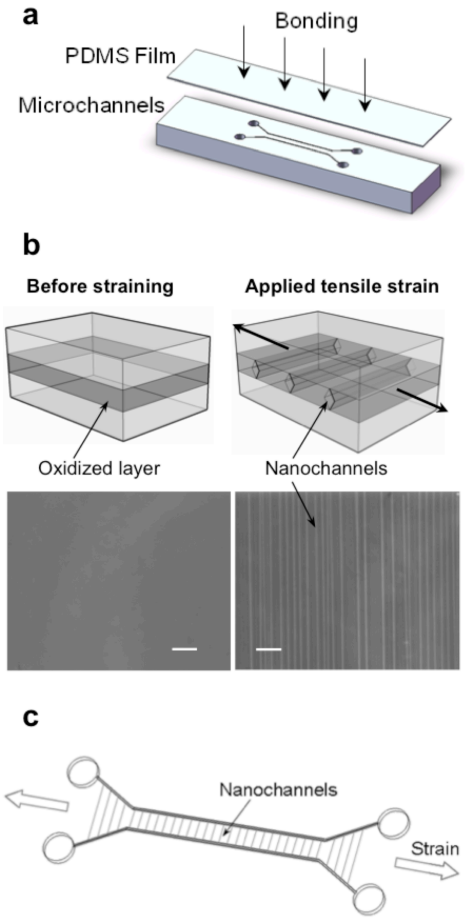

Figure 1. Fabrication and verification of adjustable nanochannels. a. A patterned PDMS substrate and a featureless film of PDMS were exposed to plasma oxygen and bonded together (step 1). b. & c. Nanochannels (tunnel cracks) connecting the two microchannel reservoirs were created within the bonded oxidized layer in response to a tensile strain (step 2). All scale bars are 25 μm.

After a preparatory step to wet the nanochannels (see Supplementary Information), fluid flow was induced electrokinetically by the application of an electric field (DC regulated power supply, BK Precision). Two solutions containing fluorescently-labeled components were visualized: a solution of fluorescein isothiocyanate (FITC)–dextran (molecular weight = 500,000 Da, Sigma-Aldrich) with peak excitation and emission wavelengths in fluorescence imaging of 480 and 535 nm, respectively, and a suspension of single quantum dots (Qdot 605 Streptavidin Conjugate, Molecular Probes, Invitrogen), which were fluorescently imaged with peak excitation and emission wavelengths of 425 and 605 nm, respectively. Electrochemical measurements were made using a picoammeter (Model 6487 Picoammeter/Voltage Source, Keithley Instruments, Inc.) in ohms-measurement mode with an applied voltage of 0.1 V. The electrolyte was 0.1 M potassium chloride (KCl) and the probes were silver/silver chloride (Ag/AgCl) pellet electrodes (EP1, World Precision Instruments).

Results and Discussion

Tunnel Cracking

Upon applying a uniaxial tensile strain to the device, an array of parallel tunnel cracks[21] was produced. These were observed optically in phase-contrast, transmitted-light mode. The first cracks were observed when the applied strain reached about 5%. Continuous increase of the applied tensile strain increased the density of cracks, in agreement with prior cracking studies on a similar system[22], so that at a strain of 25%, the average spacing between the cracks was 3.3 ± 1.2 μm. The tunnel cracks ran across the specimen, functioning as nano-channels, connecting the pre-fabricated reservoirs (Fig. 1c). Furthermore, by ensuring that the featureless PDMS was sufficiently thin, it was possible to produce high-magnification optical images of the nano-channels and their contents. These optical observations, although not quantitatively resolvable, also indicated that the width of the cracks increased with strain.

Upon relaxing the strain, the cracks collapsed and appeared to heal. Subsequent re-loading caused the original cracks to open again. As will be discussed further in a subsequent section, it was apparent that this system was one in which the cross-sectional dimensions of the channels could be changed from fully open to completely closed simply by applying or removing a uniaxial tensile strain. First, however, the ability to induce flow and control flow rates through statically opened nanochannels was verified.

Flow characterization via continuous and discrete fluorescence detection

Flow through the open nanochannels was verified by investigating the electrokinetic transport of fluorescein molecules between the two reservoirs (Fig. 2a). One reservoir was loaded with pure deionized water and the other was loaded with a fluorescein solution. An electric field of 32 V/cm was applied between the two reservoirs. Upon the application of approximately 10% tensile strain, the fluorescein solution began to flow through the nanochannels. Time-lapse optical micrographs were taken of the outlet microchannel reservoir; intensity measurements from these micrographs, averaged over the center quarter area of the micro-channel, showed an increase with time in the concentration of the fluorescein solution in the outlet micro-channel (Fig. 2b). This confirmed that the tunnel cracks spanned a relatively long distance of 1 mm between the reservoirs and formed nano-channels through which flow could be induced.

Confirmation of the ability to control the flow rate and, hence, transport rate through the opened nanochannels was provided by measuring the velocity of quantum dots as a function of the magnitude of the applied electric field. A solution containing deionized water with a suspension of quantum dots was injected into both reservoirs. A tensile

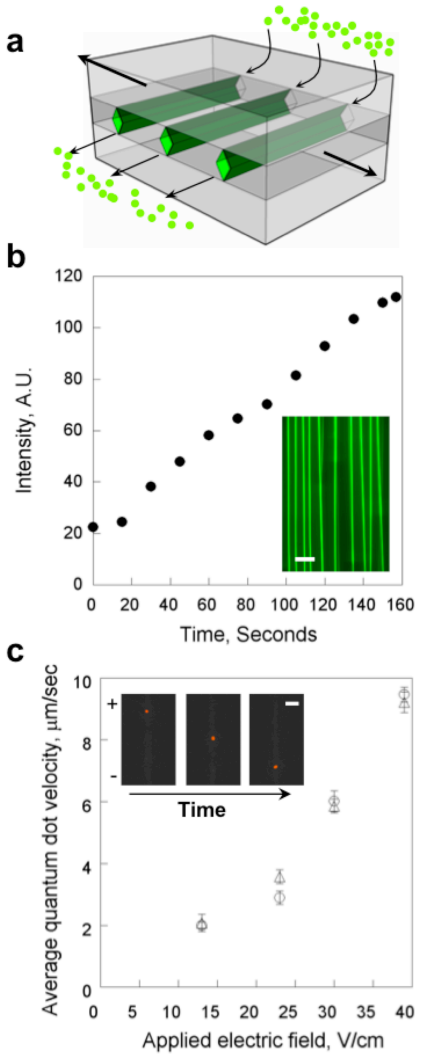

Figure 2. Verification of transport within the nanochannels. a. Fluorescein molecules were electroosmotically driven through the nanochannels from an inlet to an outlet microchannel under an electric field of 32 V/cm and an applied tensile strain of 10%. b. Fluorescence intensity measurements at the outlet reservoir increased steadily as the solution flowed from one microchannel to the other. c. The average velocity of quantum dots that were moving in nanochannels held open at 10% strain was dependent on the magnitude of the applied electric field. The circles and triangles represent measurements from two different quantum dots. All scale bars are 25 μm.

strain of 10% was applied. The electric field was varied between 10 and 40 V/cm, and the motion of the quantum dots was recorded optically. It was observed that the quantum dots traversed the nanochannels in an intermittent fashion. It appeared that the nanochannels were sufficiently narrow that there was an adhesive interaction between the quantum dots and the walls of the nanochannels[23]. Every few microns, the quantum dots would stop and vibrate in place before moving on again at a relatively constant velocity. However, it was noted that the average velocity of the quantum dots while they were mobile increased with increasing magnitude of the electric field (Fig. 2c), and upon reversal of the electric field, the quantum dots reversed direction. The velocity of the quantum dots was on the same order of magnitude as other particles and solutions travelling under an electric field in channels of similar dimensions fabricated with other methods in silicon-based materials[24, 25] and polyimide[26]. When the applied tensile strain was relaxed to close the nanochannels, the quantum dots were trapped and did not move at all, even in the presence of an electric field.

Nanochannel cross-section adjustability

Verification of the reversible adjustability of the nanochannels was performed using electrical resistance measurements. Two baseline resistance measurements were taken before any tunnel cracks were introduced into the brittle layer. The first measurement was the resistance along a single microchannel reservoir filled with 0.1 M KCl; the measured value of 945-950 kΩ was used in conjunction with the dimensions of the microchannel to compute the resistivity of the solution to be 0.3 Ω·m. The second measurement was the resistance between the two microchannel reservoirs before fracturing the brittle layer. This resistance was determined to be between 1 and 10 GΩ, which is comparable to the resistance of a similar volume of bulk PDMS and confirmed that there was no direct connectivity between the microchannels.

A strain of 26% was then applied to form cracks, and the Ag/AgCl electrodes were inserted into diagonally opposed inlet and outlet ports. Once the cracks had filled with the electrolyte and the resistance had equilibrated, the electrical resistance across the length of the nano-channels was determined to be 1.5 MΩ. This value of resistance could be used in conjunction with the geometry, observed crack density, and resistivity of the electrolyte to deduce that the average cross-sectional area of the nanochannels was about 0.505 μm^2 in this fully-strained case.

The strain was then relaxed in increments of 2.6%, with each relaxed strain being held for 2 minutes before the resistance across the nanochannels was measured. Figure 3 shows how the resistance increased monotonically by nearly two orders of magnitude as the strain was decreased, to 115 MΩ when the system was completely relaxed. This increase in resistance was associated with a decrease in the cross-sectional area of the channels as the strain was reduced. While no cracks could be observed optically after the strain had been relaxed, it was noted that the resistance continued to increase for about an hour after the strain had been completely removed, until eventually reaching a level comparable with the uncracked PDMS (Fig. 3). This indicates that, while too small to be visible optically, cracks were still present immediately after the strain had been completely removed, and then healed over a period of time. Such healing is expected to occur in these small-scale systems owing to the presence of surface forces, but the process is clearly limited kinetically by the requirement that the last remnants of the liquid be forced out of the cracks before complete healing.

The electrical resistance measured immediately after the strain was completely removed can be used to estimate the cross-sectional area of the channels if it is assumed that the crack density remains constant during the unloading process (*i.e.*, while cracks may shrink so that they are not optically visible, they do not heal completely until the strain is

completely removed). This calculation indicates an average cross-sectional area of about 7 x 10^3 nm^2 per channel immediately after complete unloading. However, the optical observations suggested that some cracks collapsed to at least below the level of optical detection as the strain was removed, while some remained wide enough to be visible optically.

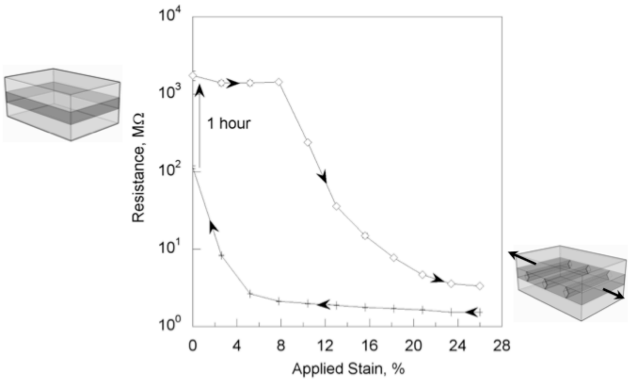

Figure 3. Verification of the adjustability of the nanochannels. The channels were filled with a 0.1 M KCl solution and electrical resistance measurements were taken across them as the applied strain was varied. At each step in applied strain, the system was allowed to equilibrate for 2 minutes before recording the resistance measurements corresponding to the markers on the graph.

Upon re-applying the strain, no change in resistance was observed until a strain of about 10%, when the resistance began to decrease again, and, as noted above, the cracks re-appeared at the same location of the original cracks. That the healed cracks re-open upon the re-application of tensile strain is a reflection of the the view that they are held together by surface forces (as opposed to healing by the formation of chemical bonds). This preserves the hydrophilic crack surfaces during the healing and re-opening cycle, and ensures that a particle trapped in a healed crack is released upon re-application of the strain. The delay of their re-opening is consistent with the fracture mechanics perspective that a critical strain-energy release rate is required to re-propagate even a single crack in a healed array of cracks. Since there is very little time-dependence of PDMS[16], the hysteresis between the loading and unloading resistance curves is probably associated with fluid flow in the nanochannels. Subsequent unloading and loading curves showed that the general form of the curve and the magnitude of the resistance measurements were repeatable.

Conclusions

In conclusion, we have used the fracture properties of a brittle sandwich layer in an elastomer to generate nanochannels that open and close reversibly upon the application of a tensile strain. While fracture is a phenomenon that is usually associated with failure, we have shown here how it can be used as a simple and low cost fabrication procedure to create nanochannels. This technique, combined with a robust and versatile operation enabled by reversible adjustability of the channel cross-sections, not only expands the range of possible nanochannel experiments, but also brings the ability to perform such nanochannel experiments to any lab.

Acknowledgements

We thank Nicholas Douville for help with the electrical resistance measurements and the NIH (grants HG004653 and EB003793) for support.

Notes and references

[a] *Mechanical Engineering, University of Michigan, Ann Arbor, USA. Fax: (734) 647-3170; Tel: (734) 763-5289; E-mail: thouless@umich.edu*
[b] *Biomedical Engineering, University of Michigan, Ann Arbor, USA. Fax: (734) 936-1905; Tel: (734) 615-5539; E-mail: takayama@umich.edu*
[c] *Macromolecular Science and Engineering, University of Michigan, Ann Arbor, USA.*
[d] *Materials Science and Engineering, University of Michigan, Ann Arbor, USA.*

1 K. B. Jirage, J. C. Hulteen and C. R. Martin, *Science*, 1997, **278**, 655-658.
2 S. B. Lee, D. T. Mitchell, L. Trofin, T. K. Nevanen, H. Soderlund and C. R. Martin, *Science*, 2002, **296**, 2198-2200.
3 S. M. Stavis, J. B. Edel, K. T. Samiee and H. G. Craighead, *Lab Chip*, 2005, **5**, 337-343.
4 J. T. Mannion, C. H. Reccius, J. D. Cross and H. G. Craighead, *Biophys. J.*, 2006, **90**, 4538-4545.
5 C. H. Reccius, J. T. Mannion, J. D. Cross and H. G. Craighead, *Phys. Rev. Lett.*, 2005, **95**.
6 W. Reisner, K. J. Morton, R. Riehn, Y. M. Wang, Z. N. Yu, M. Rosen, J. C. Sturm, S. Y. Chou, E. Frey and R. H. Austin, *Phys. Rev. Lett.*, 2005, **94**.
7 R. Riehn, M. C. Lu, Y. M. Wang, S. F. Lim, E. C. Cox and R. H. Austin, *P. Natl. Acad. Sci. USA*, 2005, **102**, 10012-10016.
8 J. O. Tegenfeldt, C. Prinz, H. Cao, S. Chou, W. W. Reisner, R. Riehn, Y. M. Wang, E. C. Cox, J. C. Sturm, P. Silberzan and R. H. Austin, *P. Natl. Acad. Sci. USA*, 2004, **101**, 10979-10983.
9 B. D. Gates, Q. B. Xu, M. Stewart, D. Ryan, C. G. Willson and G. M. Whitesides, *Chemical Reviews*, 2005, **105**, 1171-1196.
10 P. Abgrall and N. T. Nguyen, *Analytical Chemistry*, 2008, **80**, 2326-2341.
11 L. M. Bellan, E. A. Strychalski and H. G. Craighead, *Journal of Vacuum Science & Technology B*, 2008, **26**, 1728-1731.
12 L. Zhang, F. X. Gu, L. M. Tong and X. F. Yin, *Microfluidics and Nanofluidics*, 2008, **5**, 727-732.
13 S. M. Park, Y. S. Huh, H. G. Craighead and D. Erickson, *P. Natl. Acad. Sci. USA*, 2009, **106**, 15549-15554.
14 S. Choi, M. Yan and I. Adesida, *Appl. Phys. Lett.*, 2008, **93**.
15 N. Bowden, W. T. S. Huck, K. E. Paul and G. M. Whitesides, *Appl. Phys. Lett.*, 1999, **75**, 2557-2559.
16 S. Chung, J. H. Lee, M. W. Moon, J. Han and R. D. Kamm, *Adv. Mater.*, 2008, **20**, 3011-3016.
17 D. Huh, K. L. Mills, X. Y. Zhu, M. A. Burns, M. D. Thouless and S. Takayama, *Nat. Mater.*, 2007, **6**, 424-428.
18 Y. N. Xia and G. M. Whitesides, *Annu. Rev. Mater. Sci.*, 1998, **28**, 153-184.
19 S. Bhattacharya, A. Datta, J. M. Berg and S. Gangopadhyay, *J. Microelectromech. S.*, 2005, **14**, 590-597.
20 F. Katzenberg, *E-Polymers*, 2005.
21 S. Ho and Z. Suo, *J. Appl. Mech.-T. ASME*, 1993, **60**, 890-894.
22 K. L. Mills, X. Zhu, S. Takayama and M. D. Thouless, *J. Mater. Res.*, 2008, **23**, 37-48.
23 G. Drazer, J. Koplik, A. Acrivos and B. Khusid, *Phys. Rev. Lett.*, 2002, **89**.
24 A. L. Garcia, L. K. Ista, D. N. Petsev, M. J. O'Brien, P. Bisong, A. A. Mammoli, S. R. J. Brueck and G. P. Lopez, *Lab Chip*, 2005, **5**, 1271-1276.
25 G. O. F. Parikesit, A. P. Markesteijn, V. G. Kutchoukov, O. Piciu, A. Bossche, J. Westerweel, Y. Garini and I. T. Young, *Lab Chip*, 2005, **5**, 1067-1074.
26 J. C. T. Eijkel, J. Bomer, N. R. Tas and A. van den Berg, *Lab Chip*, 2004, **4**, 161-163.

Graphical Contents Entry

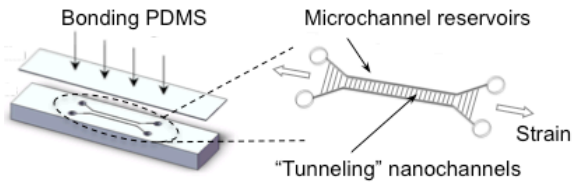

Tunnel cracking of oxidized, bonded PDMS to produce size-adjustable nanochannels in a direct and simple fashion.

5